Available online at www.sciencedirect.com
ScienceDirect
Scripta Materialia 61 (2009) 165–168
Scripta MATERIALIA
www.elsevier.com/locate/scriptamat

A re-examination of the mechanism of thermosonic copper ball bonding on aluminium metallization pads

H. Xu,[a,*] C. Liu,[a] V.V. Silberschmidt,[a] S.S. Pramana,[b] T.J. White[b] and Z. Chen[b]

[a] *Wolfson School of Mechanical and Manufacturing Engineering, Loughborough University, Loughborough LE11 3TU, UK*
[b] *School of Materials Science and Engineering, Nanyang Technological University, Nanyang Avenue, Singapore 639798, Singapore*

Received 5 February 2009; revised 13 March 2009; accepted 17 March 2009
Available online 21 March 2009

The nanoscale interfacial characteristics of thermosonic copper ball bonding on aluminium metallization were investigated. It was found that ultrasonic vibration swept oxides of aluminium and copper from parts of the contact area, promoting the formation of intermetallic compound Al_2Cu (approx.20 nm thick). Where oxides persisted, an amorphous aluminium oxide layer connected with a crystalline copper oxide. It was estimated that ultrasonic vibration caused an effective local temperature increase to 465 °C that accelerated interdiffusion and enhanced the formation of Cu–Al intermetallics.
© 2009 Acta Materialia Inc. Published by Elsevier Ltd. All rights reserved.

Keywords: Thermosonic bonding mechanism; Interfacial structure; Intermetallic compounds

Thermosonic copper ball bonding to aluminium metallization provides excellent electrical and mechanical properties for high-speed, high-power devices and fine-pitch microelectronic applications, and may prove a cost-effective alternative to gold ball bonding [1]. The relationship between process parameters and bondability [2–5] and the reliability of bonds subjected to thermal cycling and ageing [6–11] are well studied. However, the fundamental principles of bonding remain poorly understood [12]. They are commonly described as fretting [13] or micro-slip [14,15] processes, where the former considers bonding to be promoted by interfacial sliding that cleans and heats metallization pad, while the latter predicts preferential slips and bonding at the interfacial periphery. However, neither mechanism is supported by examination of copper–aluminium boundaries at near-atomic scales.

Intermetallic formation at the Cu–Al bond should improve strength, and five alloys ($Al_2Cu(\theta)$, $AlCu(\eta_2)$, $Al_3Cu_4(\zeta_2)$, $Al_2Cu_3(\delta)$ and $Al_4Cu_9(\gamma_2)$) are possible [9], but excessive growth will degrade mechanical integrity [1,10,16]. For example, Kim et al. [10] have found that after ageing for 100 h at 250 °C, the IMC was approx.1.2 μm. The corresponding shear strength was about 80% of that in the as-bonded state and the failure site was the interface between Cu–Al IMC and SiO_2/Si. Although scanning electron microscopy (SEM) found no Cu–Al intermetallics after bonding [6,7], extremely thin alloy domains are difficult to detect with this method. Therefore, this study was undertaken to examine the interfacial characteristics of the Cu–Al boundary in fine detail.

In these experiments, a copper wire (99.99 wt.%, 25.4 μm diameter) was bonded to an aluminium metallization pad (1 μm thick) on a silicon chip using an ASM Eagle 60 ball/wedge automatic bonder at an ultrasonic frequency of 138 kHz. An electronic flame-off (EFO) process produced a spherical ball under a protective gas mixture (95% N_2 + 5% H_2) introduced at the rate of 0.8 l min^{-1}, to limit the oxidation of copper. Bonding was completed within 0.025 s using a combination of transverse ultrasonic vibration (150 mW), an external force normal to the interface (0.6 N), and heat (200 °C). Shear (180.7 MPa) and pull (68.5 MPa) tests confirmed the high strength of Cu–Al bonds. To study the interfaces in detail, region-specific transmission electron microscopy (TEM) sections of the Cu–Al interfaces were prepared using a dual-beam focused ion beam (FIB).

Cu–Al interfaces contain two types of morphologies, labelled as A and B (Fig. 1), with fractions of approx.70% and approx.30%, respectively. Both morphologies are gap-free and void-free. Here, voids signify Kirkendall voids, which were reported to be present at

* Corresponding author. Tel.: +44 1509227684; e-mail: H.Xu3@lboro.ac.uk

1359-6462/$ - see front matter © 2009 Acta Materialia Inc. Published by Elsevier Ltd. All rights reserved.
doi:10.1016/j.scriptamat.2009.03.034

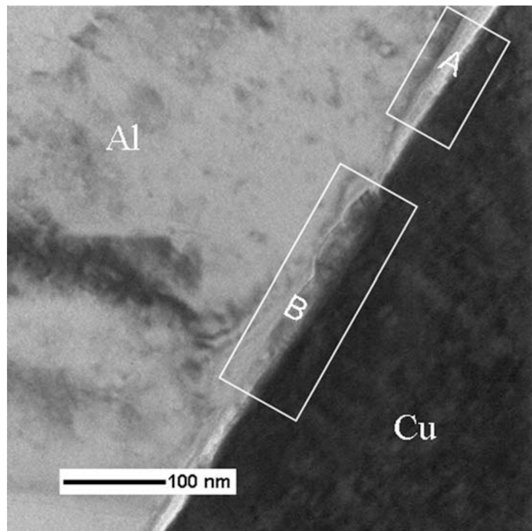

Figure 1. TEM image of interfacial morphologies of Cu–Al bond.

nanoscale at the Au/Al interface of thermosonic Au–Al bonds [17], while a gap means that two metals are not metallurgically bonded and there is a narrow and relative long area between their free surfaces. The later was found at sub-micro scale in the central contact area of thermosonic Cu–Al bonds in our previous study when the bonding parameters were not optimized. In region A three layers can be distinguished, with those closest to aluminium being amorphous (A-1 and A-2), while layer A-3 abutting copper is crystalline (Fig. 2a). Scanning (S)TEM–energy dispersive X-ray spectrometry (EDX) suggests A-1 is aluminium oxide and A-2 was an aluminium-rich phase (Table 1). Since a compact oxide film with thickness 5–20 nm forms on the aluminum in air [18], the lay of amorphous alumina with 10–15 nm thick (A-1, Fig. 2a) is believed to exist before bonding and not be removed during bonding.

In detail, region A-A in Figure 2a consists of two distinct electron interference patterns (Fig. 2b) with fast Fourier transform (FFT) analysis of these regions consistent with copper metal (*Fm*-3*m*, $a = 0.361$ nm) and CuO ($C12/c1$, $a = 0.465$ nm, $b = 0.341$ nm, $c = 0.511$ nm, $\beta = 99.59°$) in agreement with STEM–EDX (Table 1). The copper oxide (approx.3 nm thick) is thought to form during electronic sparking and ball formation. The amorphous aluminium oxide and copper oxide layers appear contiguous at the atomic scale.

In the second type of Cu–Al interface (region B, Fig. 1) the amorphous aluminium oxide was replaced with a layer (approx.20 nm thick) (Fig. 3a), which is crystalline (Fig. 3b and c). FFT analysis of the interference lattices are consistent with Al_2Cu (*I4*/*mcm*, $a = 0.496$ nm, $b = 0.859$ nm and $c = 0.848$ nm) aligned along [2 1 0] orientation forming a boundary with Al (*Fm*-3*m*, $a = 0.406$ nm) and Cu (*Fm*-3*m*, $a = 0.361$ nm) in [1 0 1] (Fig. 3b and c). The interfaces may be semi-coherent as Al $d_{020} = 0.203$ nm, $d_{11-1} = 0.234$ nm; Al_2Cu $d_{002} = 0.244$ nm, and $d_{-121} = 0.237$ nm, but a selection of images collected over a range of tilt angles would be required for confirmation.

Since continuous and compact layers of aluminium oxide and copper oxide layers were present before bonding [12,19], it is now clear that ultrasonic vibration removes these from some parts of the contact area (such as region B, Fig. 1), while in the others (such as region A, Fig. 1), the oxides were persistent. The contacting surfaces are relatively rough [20], and wear preferentially at the asperities, while oxides remain in surface depressions. Where the oxides are absent, a Cu–Al intermetallic layer forms with Al_2Cu nucleating first. Murali et al. [6] and Ratchev et al. [7] did not detect Cu–Al interme-

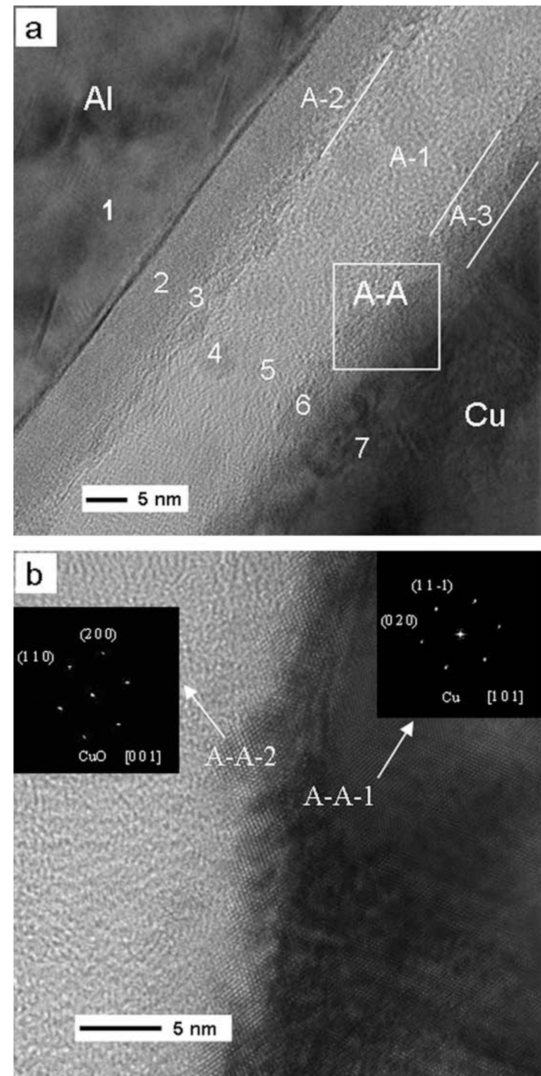

Figure 2. (a) Details of region A in Figure 1 with three layers between copper and aluminium. (b) Details of region A-A in (a): region A-A-1-Cu and region A-A-2-CuO.

Table 1. STEM–EDX results for regions 1–7 in Figure 2a.

Regions	O K (at.%)	Al K (at.%)	Cu K (at.%)
1	4.8 ± 10	93.1 ± 2	2.1 ± 2
2	11.2 ± 10	87.4 ± 2	1.4 ± 2
3	55.2 ± 10	43.0 ± 2	1.8 ± 2
4	42.5 ± 10	50.1 ± 2	7.4 ± 2
5	46.6 ± 10	48.0 ± 2	5.4 ± 2
6	44.8 ± 10	11.7 ± 2	43.5 ± 2
7	6.3 ± 10	3.3 ± 2	90.4 ± 2

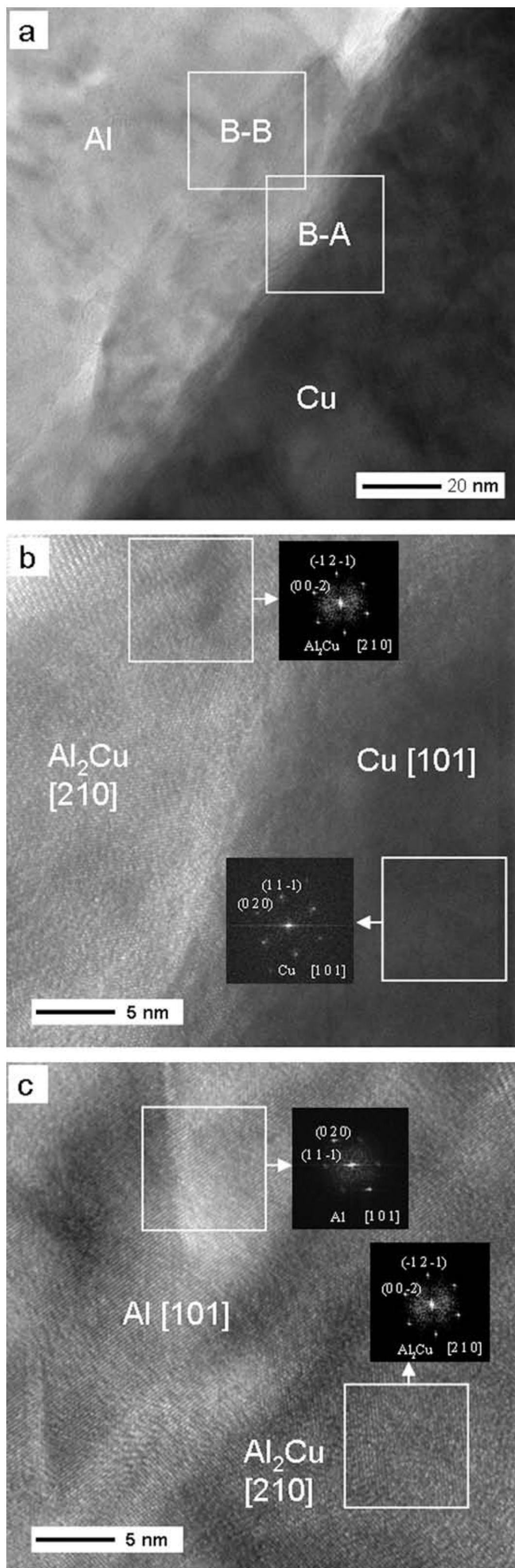

Figure 3. (a) Details of region B in Figure 1 show that the amorphous aluminium oxide layer disappears, and an approx. 20 nm thick layer of crystalline Al_2Cu introduced. (b) Details of region B-A in (a). (c) Details of region B-B in (a).

tallics by SEM due to their extremely small size, however, they can be identified by TEM.

It has been reported that intermetallic growth in Cu–Al bonds follows a parabolic law during thermal ageing [8,10,16], such that

$$x = (Dt)^{1/2} \tag{1}$$

and

$$D = D_0 \exp(-Q/RT) \tag{2}$$

where x is the IMC thickness at time t, D is the growth rate constant, D_0 is a pre-factor, Q is the activation energy, R is the molar gas constant, and T is the absolute temperature.

According to Xu et al. [8], $Q = 1.01$ eV and $D_0 = 1.21 \times 10^{-7}$ m^2 s^{-1}, for the growth of Cu–Al intermetallics. Consequently, in the present studies with $x = 20$ nm and $t = 0.025$ s, the effective (or equivalent) temperature is estimated to be 465 °C. The effective temperature includes the temperature T increase caused by mechanical vibration and a decrease in Q as a result of ultrasonic action, but the contribution of each term requires investigation. A previous in situ measurement of interfacial temperature using K-type thin film thermocouples yielded 320 °C [21]. The higher temperature estimated in this study is for a specific small local region, while the thermocouple measurement is an average over the sensor (20 μm in width). Despite the uncertainty of temperature determination at the interface, it is clear that ultrasonic vibration not only cleaned the contact surface, but also increased the effective local temperature, which improved atomic interdiffusion between Cu and Al.

To summarize, a thermosonic copper ball bonding mechanism that exploits ultrasonic vibration has been found to locally remove aluminium and copper oxides (such as region B, Fig. 1), which promotes the Cu/Al adhesion under the bonding pressure. Atomic interdiffusion proceeds in areas where the fresh metals are exposed and in contact. The flash temperature at these regions effectively increases to 465 °C due to the atomic motion induced by ultrasonic vibration. This promotes the formation of Cu–Al intermetallic (Al_2Cu) layer and significantly improves the bonding strength. In the regions where oxide remains and no intermetallics exist (such as region A, Fig. 1), the aluminium and copper oxides directly connect without voids or gaps.

This paper is an output of the PMI2 Project funded by the UK Department for Innovation, Universities and Skills (DIUS) for the benefit of the Singapore Higher Education Sector and the UK Higher Education Sector. The authors also acknowledge Dr Geoff West, Mr Shaode Zhu and Mr Honghui Wang for their advice and assistance with the experiments.

[1] S.L. Khoury, D.J. Burkhard, D.P. Galloway, T.A. Scharr, IEEE Trans. Comp. Hybrids Manuf. Tech. 13 (1990) 673.
[2] J. Qi, N.C. Hung, M. Li, D. Liu, Scripta Mater. 54 (2006) 293.
[3] Y. Ding, J.K. Kim, P. Tong, Mech. Mater. 38 (2006) 11.
[4] L.T. Nguyen, D. McDonald, A.R. Danker, P. Ng, IEEE Trans. Comp. Pack. Manuf. Tech. 18 (1995) 423.

[5] A. Shah, M. Mayer, Y. Zhou, S.J. Hong, J.T. Moon, Microelectron. Eng. 85 (2008) 1851.
[6] S. Murali, N. Srikanth, C.J. Vath, Mater. Res. Bull. 38 (2003) 637.
[7] P. Ratchev, S. Stoukatch, B. Swinnen, Microelectron. Reliab. 46 (2006) 1315.
[8] H. Xu, C. Wang, C. Hang, Acta Metall. Sin. 43 (2007) 125.
[9] C. Xu, T. Sritharan, S.G. Mhaisalkar, Scripta Mater. 56 (2007) 549.
[10] H.J. Kim, J.Y. Lee, K.W. Paik, K.W. Koh, W.J.S. Choe, J. Lee, J.T. Moon, Y.J. Park, IEEE Trans. Comp. Pack. Tech. 26 (2003) 367.
[11] S. Murali, N. Srikanth, C.J. Vath, Mater. Lett. 58 (2004) 3096.
[12] G.G. Harman, Wire Bonding in Microelectronics, Materials, Processes, Reliability, and Yield, second ed., McGraw-Hill, New York, 1997.
[13] A.P. Hulst, Weld. J. 57 (1978) 19.
[14] R.D. Mindlin, J. Appl. Mech-T ASME 18 (1951) 331.
[15] G.G. Harman, J. Albers, IEEE Trans. Parts Hybrids Pack. 13 (1977) 406.
[16] W.B. Lee, K.S. Bang, S.B. Jung, J. Alloy Comp. 390 (2005) 212.
[17] A. Karpel, G. Gur, Z. Atzmon, W.D. Kaplan, J. Mater. Sci. 42 (2007) 2334.
[18] G.E. Totten, D.S. Markenzie, Handbook of Aluminum, vol. 1: Physical Metallurgy and Processes, Routledge, New York, 2003.
[19] S.K. Prasad, Advanced Wirebond Interconnection Technology, Springer Verlag, New York, 2004.
[20] G. Pugliese, S.M.O. Tavares, E. Ciulli, L.A. Ferreira, Wear 264 (2008) 1116.
[21] J. Ho, C. Chen, C. Wang, Sens. Actuat. A-Phys. 111 (2004) 118.